Theoretical study of Na adsorption on top of In chains on the Si(111) surface

Jun-Hyung Cho, Dong-Hwa Oh, and Leonard Kleinman
Department of Physics, University of Texas, Austin, Texas 78712-1081
(Received 22 April 2002; published 29 August 2002)

The adsorption of Na on In-adsorbed Si(111) surfaces is investigated by first-principles density-functional calculations. Charge transfer from Na atoms to the p_z orbitals of neighboring In atoms occurs, indicating ionic bonding between Na atoms and In chains. Although a repulsive interaction between adsorbed Na atoms exists, adsorption on every (two inequivalent) hollow site between In chains can be attained at saturation coverage. Based on our results for the atomic and electronic structures of Na adsorbates on In/Si(111), we discuss recent low-energy electron diffraction, scanning tunneling microscopy, and electron energy loss spectroscopy data. In particular, we find that the (4×2) Na chains observed at low coverage are slightly energetically unfavorable and speculate that they are a consequence of growth kinetics.

DOI: 10.1103/PhysRevB.66.075423 PACS number(s): 68.35.Bs, 68.35.Rh, 73.20.−r

I. INTRODUCTION

Impurities in a crystal alter the local electronic distribution; valence electrons screen charged impurities, producing an attenuated charge density wave (CDW) or Friedel oscillation near the impurity site.[1] This local charge rearrangement will generate forces on the ion cores, consequently breaking the local symmetry and possibly causing a change in the short-range ionic order. This scenario has been demonstrated on the Sn/Ge(111) surface in which upon cooling a phase transition from the $\sqrt{3}\times\sqrt{3}$ to 3×3 symmetry was observed.[2] Here Ge substitutional defects which act as local impurities nucleate the 3×3 superstructure for a few unit cells even above the transition temperature.[3]

Recently at room temperature, using low-energy-electron diffraction (LEED), scanning tunneling microscopy (STM), and high-resolution electron-energy-loss spectroscopy (HREELS), Lee *et al.*[4] reported the observation of a local impurity-derived Peierls-like reconstruction on a quasi-one-dimensional (quasi-1D) system [i.e., the In/Si(111) surface] from the 4×1 to the 4×2 structure. They used Na adsorbates as impurities. According to their LEED analysis, the disordered 4×2 structure domain begins to appear at around $\theta=0.2$ ML and the 4×2 long-range order is best developed at 0.4 ML. Since Lee *et al.* defined $\theta=1$ to be that coverage which causes the work function to be a minimum, it is not clear whether $\theta=1$ means that one or both of the bonding sites are supposedly occupied in the 4×1 unit cell. We suspect they mean one is, and to avoid confusion, we will adopt that convention. We will find that this is consistent with our calculated work functions for $\theta=0$, 1/3, 0.5, 1, and 2 ML. Even at a low coverage of less than 0.1 ML the filled-state STM image showed local 4×2 short-range order where bright spots appear around Na adsorbates along the In chain direction. Since these bright spots are separated mostly with a 4×2 periodicity and resemble those of the low-temperature reconstruction of the clean In/Si(111)-(4×2) surface, they interpreted the observed 4×2 STM image to be caused by the Na-induced local charge density modulation along the In chain direction. Initially, the origin of the phase transition from the 4×1 to the 4×2 structure at the In/Si(111) surface where it occurs below 100 K was suggested to be a 1D CDW along the In chain.[5] However, this is not supported by subsequent x-ray diffraction experiments[6] and first-principles calculations.[7] The HREELS data for the Na-induced 4×2 structure showed two loss peaks at energies of 105 ± 8 meV and ~1100 meV.[4] Lee *et al.* attributed the lower loss energy to the interband transition between the split bands (generated by the CDW gap) at the Fermi energy, but could not identify the bands associated with the other peak.

In this paper we study the adsorption of Na on In/Si(111) surfaces using first-principles density-functional theory calculations. The potential energy surface mapped out by the adsorption energies calculated at different positions on the In/Si(111) surface has minima along the 1D channel between the two zigzag In chains. The activation barrier for diffusion of a Na atom between these energy minima is only ~0.1 eV, resulting in easy formation of 1D Na wires. Here we predict that the formation of a 4×2 structure is preferred over the 4×1 at low coverages because of repulsion between adsorbed Na atoms, in accordance with the LEED analysis. The calculated electronic structure of the 4×2 Na wire does not support the metal-insulator transition claimed by the EELS data of Lee *et al.*,[4] but shows gaps opening along the $\Gamma X'$ and $M'Y$ symmetry lines. Our simulated STM image for the 4×2 Na wire shows a single bright spot per Na atom, qualitatively similar to the observed one. Our results of the potential energy surface, surface-state energy bands, and simulated STM images lead us to believe that the 4×2 order observed by the LEED and STM is not caused by a CDW around the Na adsorbate, but represents a 4×2 Na line which has a finite length at low coverages.

The paper is organized as follows. In Sec. II the calculational method is described. In Sec. III we present our results of the structural and electronic properties of 1D Na wires with various coverages and discuss recent experimental data. Finally, conclusions are given in Sec. IV.

II. CALCULATIONAL METHOD

We perform the total-energy and force calculations by using density-functional theory[8] within the generalized-

gradient approximation.[9] All atoms are described by norm-conserving[10] pseudopotentials in the separable form of Kleinman and Bylander.[11] The surface is modeled by a periodic slab geometry. Each slab contains six Si atomic layers (not including the Si surface chain) plus adsorbed In and Na layers and the the bottom Si layer is passivated by one H atom per Si atom. The thickness of the vacuum region between these slabs is about 10 Å. The electronic wave functions are expanded in a plane-wave basis set with a cutoff energy of 15 Ry. The **k**-space integrations are done with meshes of 48, 24, and 16 **k** points in the (4×1), (4×2), and (4×3) surface Brillouin zones, respectively. The position of all atoms, except the innermost Si layer atoms, held at their calculated bulk positions ($a_0=5.47$ Å), are allowed to relax along the calculated Hellmann-Feynman forces until all the residual force components are less than 1 mRy/bohr.

Because we use standard periodic boundary conditions and because the two surfaces of our film have different work functions, we can only estimate the work function on either side. When the two sides of the film are identical, one merely subtracts the Fermi energy from the planar average of the Coulomb potential at the midpoint between films to obtain the work function. The planar average of the Coulomb potential attains a constant value well before the midpoint.[12] When the two surfaces have different work functions, there is a constant electric field between the films. When we subtract off the Coulomb potential at the midpoint between the two outermost planes of atoms, we obtain an average of the two work functions. This average is not exact because the midpoint is not unique; e.g., the midpoint could have been chosen between planes where the charge density falls to some fraction of its average interior value. The determination of the individual work functions requires determining the potential difference between the two ill-defined points where the film potentials stop and the electric field begins. To minimize this error we obtained the hydrogenated surface work function for the case with the smallest potential difference (clean In surface) and used that to obtain the In/Na surface work functions. It is ironic that the seminal self-consistent thin film calculations[13] used infinite wall boundary conditions which avoid these problems altogether, but all calculations of which we are aware since then (except those expanding in localized orbitals) have used periodic boundary conditions.

III. RESULTS

To find plausible adsorption sites of Na on the In/Si(111) surface, we calculated the adsorption energy defined as

$$E_{\mathrm{ads}}=(E_{\mathrm{InSi}}+nE_{\mathrm{Na}}-E_{\mathrm{Na/InSi}})/n, \tag{1}$$

where E_{InSi} and $E_{\mathrm{Na/InSi}}$ are the total energies of slabs with clean and Na-adsorbed In/Si(001) surfaces, respectively. E_{Na} is the total energy of a spin-polarized free Na atom and n denotes the number of adsorbed Na atoms. We consider 27 different adsorption sites in half of the 4×1 unit cell [see Fig. 1(a)]. Here, we use the large 4×2 unit cell to make negligible the interaction between adsorbed Na atoms and relax only the height of Na atoms while keeping In and Si atoms fixed at the positions of a relaxed In/Si(111)-(4×1) surface. The relaxation effect of the In/Si(111) substrate will be shown to be negligible for the relative energies of different adsorption sites at the same coverage (see Table I). The potential-energy surface obtained by the calculated adsorption energies is displayed in Fig. 2. We find that the two hollow sites (H_1 and H_2 in Fig. 2) between the two In chains are the most stable sites with adsorption energies of 1.376 and 1.372 eV, respectively. In Fig. 2 we also see the zigzag valley row along the Si zigzag chain. The hollow site H_3 (H_4) in this row is less stable than the H_1 site by an adsorption energy of about 0.20 (0.25) eV. Note that there is an energy barrier of about 0.35 eV for the diffusion path from H_3 to H_1. Using an Arrhenius-type activation process with a typical value[14] ($\sim10^{14}$ Hz) for the preexponential factor the diffusion rate from H_3 to H_1 is estimated as $\sim1.35\times10^8$ s^{-1} at room temperature. Thus, we expect that 1D Na wires can be easily formed along the channel between the two zigzag In chains.

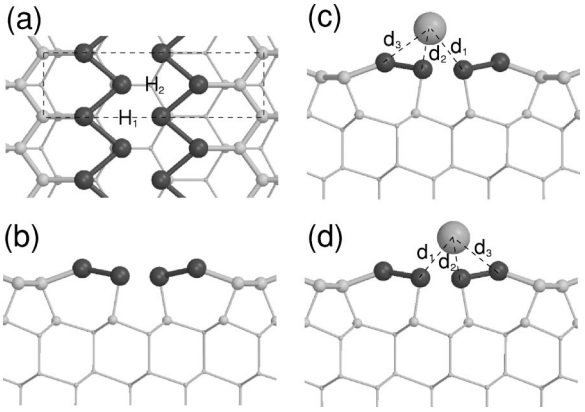

FIG. 1. Equilibrium structure of the In/Si(111)-(4×1) surface: (a) the top view and (b) the side view. The (4×1) unit cell is indicated by the dashed line in (a). The two adsorption sites (H_1 and H_2) of Na adsorbed on In/Si(111) are marked in a 4×1 unit cell in (a). The side views of the H_1 and H_2 adsorption structures are given in (c) and (d), respectively. The distances between the Na atom and neighboring In atoms are denoted by d_1, d_2, and d_3. Note there are two d_2 neighbors. The large, medium, and small circles represent Na, In, and Si atoms.

Next we determine the atomic structures of adsorbed Na atoms at the H_1 and H_2 sites for various coverages, ranging from $\theta=1/3$ ML to 2 ML. Here we fully relax the positions of both the adsorbed Na atoms and In/Si(111) substrate. The calculated work functions for $\theta=0$, 1/3, 0.5, 1, and 2 ML are listed in Table II. One sees that they are consistent with the minimum work function occurring at or somewhat above $\theta=1$ ML.[4] We estimate the accuracy of the work functions to be 0.2 eV but the relative accuracy among the $\theta=0.5$, 1, and 2 cases to be 0.05 eV. The calculated adsorption energies for various coverages are given in Table I, together with the distances between the Na atom and the four neighboring In atoms [i.e., d_1, d_2, and d_3 in Figs. 1(c) and 1(d)]. Note from Figs. 1 and 2 that there are two d_2 neighbors. We find that the adsorption energy decreases with increasing coverage, indicating a repulsive interaction between adsorbed Na at-

TABLE I. Calculated adsorption energy (per adsorbed atom) of Na adsorbed on In/Si(111) surfaces with various coverages. The values in parentheses represent the results obtained using the fixed substrate where the positions of In and Si atoms are the same as those of a relaxed In/Si(111)-(4×1) surface. The distances d_1, d_2, and d_3 between the adsorbed Na atom and the neighboring In atoms [see Figs. 1(c) and 1(d)] are also given. For the H_1 and H_2 4×2 structure the values of the two different d_2 neighbors are given.

Site	Unit cell	θ(ML)	E_{ads} (eV)	d_1 (Å)	d_2 (Å)	d_3 (Å)
H_1	4×1	1	1.177 (1.167)	3.32	3.20	3.39
	4×2	0.5	1.424 (1.376)	3.23	3.23	3.43
	4×3	1/3	1.452	3.22	3.24	3.44
H_2	4×1	1	1.156 (1.147)	3.29	3.21	3.35
	4×2	0.5	1.420 (1.372)	3.18	3.25	3.40
	4×3	1/3	1.446	3.21	3.28	3.43
H_1 & H_2	4×1	2	1.115	3.86; 3.75	3.40; 3.39	3.31; 3.29
	4×2	1	1.127	3.39; 3.32	3.09,3.37; 3.09,3.39	3.22;3.23
	4×3	2/3	1.383	3.15; 3.17	3.18; 3.23	3.40; 3.42

oms. For the H_1 site the adsorption energy difference between the 4×3 (1/3 ML) and the 4×2 (0.5 ML) structure is only $\Delta E_{ads}=0.028$ eV, whereas the one between the 4×2 (0.5 ML) and the 4×1 ($\theta=1$ ML) structure is $\Delta E_{ads}=0.247$ eV. This trend is also shown for the H_2 site at which the adsorption energy is slightly smaller than that of the H_1 site (see Table I). Considering that this energy difference is much smaller than the magnitude of the adsorption energy, one might expect that the 4×3, 4×2, and 4×1 structures will be sequentially formed with increasing Na coverage. As a result, for 1/3 ML$<\theta<$0.5 ML (0.5 ML $<\theta<$1 ML) both the 4×3 and the 4×2 structure (4×2 and the 4×1) should coexist. Note however that the H_1 and H_2 4×3 structure[15] has a greater adsorption energy than 1/3 of the surface in the H_1 4×1 structure and 2/3 in the H_1 4×2 which also has $\theta=2/3$. This expectation is not in agreement with the LEED analysis[4] where the LEED pattern originating from the 4×2 structure starts to grow quickly when the Na coverage exceeds 0.2 ML (rather than 0.33 ML) and it is best developed at 0.4 ML. The explanation for the LEED pattern showing the indium 4×1 structure and isolated Na 4×2 structures to the exclusion of Na 4×3 and isolated Na structures could be growth kinetics. A sodium at an H_1 (H_2) site strains the indium chain so that the neighboring H_1 (H_2) sites become more attractive to other Na atoms. At a second-neighbor end site this attractive interaction may actually become larger than the Coulomb repulsion which is smaller at the end of the chain than in the interior; thus the energy barrier for escape to a neighboring H site is raised, allowing the formation of the 4×2 structure.[16] Note that the 4×1 structure with $\theta=2$ ML where Na atoms occupy both the H_1 and H_2 sites has $E_{ads}=1.115$ eV and therefore the saturation coverage of 2 ML is easily attained as the ground state for Na adsorbates on In/Si(111).

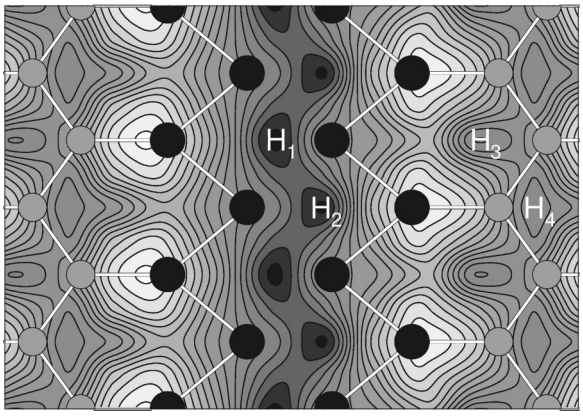

FIG. 2. Potential-energy surface for Na overlayer (0.5 ML) on the In/Si(111)-(4×1) surface. The contour spacings are 0.05 eV. The local minima points are represented by H_1, H_2, H_3, and H_4. The dark and gray circles represent In and Si atoms, respectively.

Our previous calculations[7] for the clean In/Si(111)-(4×2) surface found that the outer In atoms are displaced alternatively to form pairs, i.e., (In_1,In_2) and (In_7,In_8). For the labeling of In atoms, see Fig. 3. The distances of the paired In atoms are reduced to $d_{In_1\text{-}In_2}=3.59$ Å and $d_{In_7\text{-}In_8}=3.60$ Å, compared with the corresponding distance of 3.87 Å in the clean In/Si(111)-(4×1) surface. However, upon Na adsorption such a paring of the outer In atoms disappears to yield $d_{In_1\text{-}In_2}=3.87$ Å and $d_{In_7\text{-}In_8}=3.84$ Å. For the clean In/Si(111)-(4×2) surface the In-In bond lengths of the left-hand (right-hand) In chain are 3.01, 3.03, 3.05, and 3.09 Å along the positive (negative) **x** direction, but for the Na adsorbed 4×2 surface those bond lengths show a large difference between the left and right In chains (see Fig. 3). This is

TABLE II. Average work function of the hydrogenated and In-Na surfaces of the film and the estimated In-Na surface work function for five Na coverages defined in the text. For $\theta=1/3$, 0.5, 1 ML the H_1 adsorption site was chosen.

θ	Average	In-Na
0	4.206 eV	3.89 eV
1/3	3.818 eV	3.12 eV
0.5	3.546 eV	2.57 eV
1	3.318 eV	2.12 eV
2	3.497 eV	2.47 eV

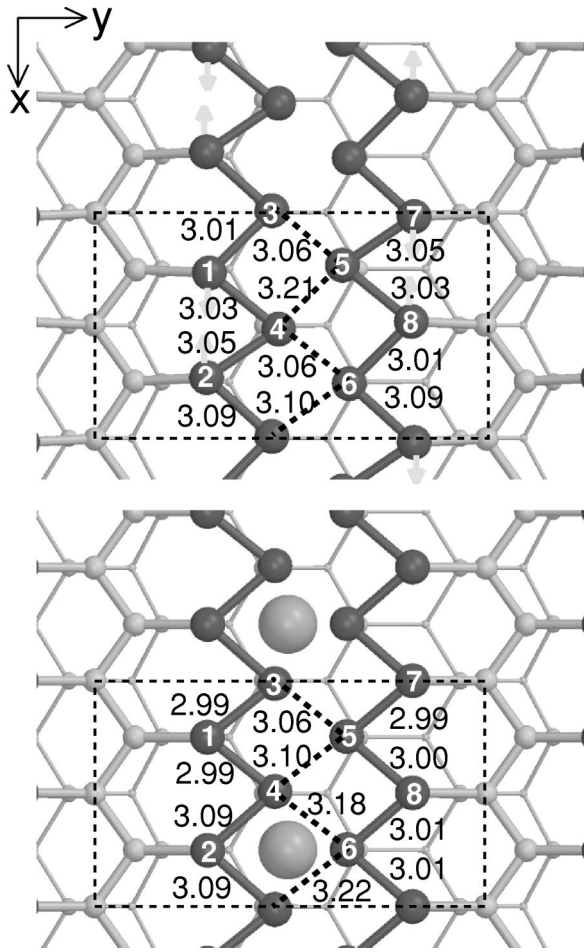

FIG. 3. The top view of the optimized structure of the clean In/Si(111)-(4×2) surface and the Na-adsorbed 4×2 surface. The *x* and *y* directions are $[\bar{1}10]$ and $[11\bar{2}]$, respectively. The arrows show pairing patterns of the outer indium atoms on the clean surface. The interatomic distances between In atoms are given in Å.

induced by the stretching of the In interchain bonds ($d_{\mathrm{In_4\text{-}In_6}}$ and $d_{\mathrm{In_3\text{-}In_6}}$) around the Na atoms.

At a low coverage of less than 0.1 ML the filled-state STM images of Lee *et al.*[4] showed the local 4×2 short-range order around Na adsorbates, where the bright spots are well separated with a 4×2 periodicity along the In chain direction. They claimed that the observed STM images manifest the Na-induced local charge modulation (i.e., a short-range CDW). They also reported that such a Na-induced CDW was fully developed even at high coverages. We simulate the STM images for 4×2 (0.5 ML), 4×1 (1 ML), and 4×1 (2 ML). The results are shown in Fig. 4. Here the filled-state (empty-state) images mapping the electron density integrated over an energy range between the Fermi energy E_F and E_F-1 (+1) eV are taken at about 2.3 Å above the Na atom (1 V was the voltage at which the experimental data[4] were taken). The filled-state [Fig. 4(a)] and empty-state [Fig. 4(b)] images of 4×2 (0.5 ML) show a single bright spot per Na atom. The bright image in the filled-state case is somewhat displaced toward three of the four neighboring In atoms. The pattern of our simulated filled-state STM images

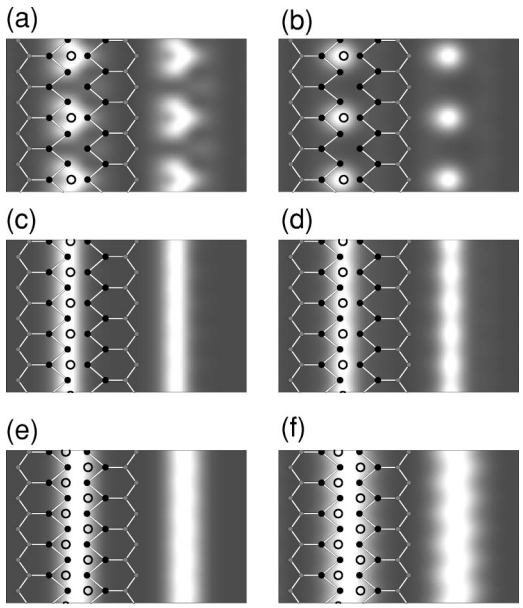

FIG. 4. Simulated filled-state and empty-state STM images of Na-adsorbed In/Si(111) surfaces with respect to the Na coverage. The filled-state [empty-state] images for 0.5 ML, 1 ML, and 2 ML are given in (a), (c), and (e) [(b), (d), and (f)]. The filled-state (empty-state) image is obtained by integrating the charge from Fermi level E_F to $E_F-1.0(+1.0)$ eV. The images were obtained at 2.3 Å above the Na atoms.

for 4×2 (0.5 ML) agrees well with that of the experimental STM data, but the detailed shapes of the bright spots cannot be compared to each other because of the low experimental resolution in Ref. 4. For the filled-state and empty-state images of 4×1 (1 ML) and 4×1 (2 ML) there is a superposition of the bright spots, producing a 1D line pattern along the In chain direction [see Figs. 4(c) and 4(d) for 1 ML and Fig. 4(e) and 4(f) for 2 ML].

In their HREELS spectra from the Na-adsorbed 4×2 surface Lee *et al.*[4] observed a significant decrease of the linewidth of the elastic peak which originates from the continuum of interband transitions near the Fermi energy, causing them to conclude that a metal-insulator transition was induced by Na adsorbates. They also found a loss peak (S_c) at a loss energy of 105±8 meV with a linewidth of 73±30 meV. This peak grows in intensity with increasing Na coverage and becomes dominant near $\theta=0.4$ ML where the 4×2 surface is best developed. Thus, they believed that the peak S_c is related to the formation of the Na-induced CDW gap. An additional loss peak (S_2) was measured at a loss energy of ~1100 meV. It is notable that the peak S_2 is at a higher loss energy than the S_1 peak (at ~750 meV) observed on the clean In/Si(001)-(4×1) surface.

In order to provide the theoretical basis for the interpretation of the above-mentioned HREELS peaks, we calculate the band structures for the Na-adsorbed 4×2 (0.5 ML) and 4×1 (1 ML) surfaces. For both surfaces the H_1 adsorption site was chosen. The calculated surface-state energy bands of 4×2 and 4×1 are shown in Figs. 5(a) and 5(b), respectively. Here we find that the dispersions of the surface-state bands are very similar to those of the corresponding clean

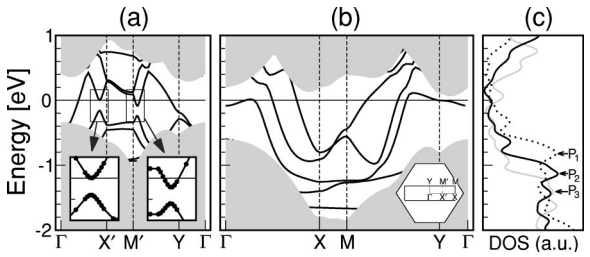

FIG. 5. Surface band structure of Na-adsorbed (a) 4×2 ($\theta=0.5$ ML) and (b) 4×1 ($\theta=1$ ML) surfaces. The energy is given relative to the Fermi energy. The two insets in (a) magnify the calculated energy levels, and the inset in (b) shows the surface Brilloin zone for the (4×1) and (4×2) unit cells with that for the (1×1) unit cell as a reference. Shaded areas are the projected bulk-band structure. (c) Density of states of the clean In/Si(111)-(4×1) (dotted line), Na-adsorbed 4×2 (black solid line), and Na-adsorbed 4×1 (gray solid line) surfaces.

In/Si(111)-(4×2) and In/Si(111)-(4×1) surfaces,[7] except that the Fermi energy rises by simply filling the In-derived surface bands. Therefore, the density of states (DOS) of the Na-adsorbed 4×2 (4×1) surface shifts to a lower energy relative to the Fermi energy [see Fig. 5(c)]. For the clean In/Si(111)-(4×1) surface the high DOS peak denoted by P_1 in Fig. 5(c) is located at 810 meV below the Fermi energy, whereas for the Na-adsorbed 4×2 (4×1) surface the corresponding peak P_2 (P_3) is at 1130 (1410) meV. These peaks originate from the flatband character of the In-derived surface states [see Fig. 2(a) of Ref. 7 and Fig. 5(b)]. Since the positions of P_1 and P_2 as well as the energy difference between these two peaks are quite comparable to those of the loss peaks S_1 and S_2 in the HREELS data,[4] it is likely that the loss peak S_1 (S_2) stems from an interband transition contributed by the peak P_1 (P_2).

Figure 5(c) shows that near the Fermi energy the occupied DOS for the Na-adsorbed 4×2 surface decreases compared with that of the clean In/Si(111)-(4×1) surface. This decrease contributes to diminishing transitions from just below to just above the Fermi energy, consistent with the HREELS data[4] in which upon Na adsorption a wide Drude tail [with a full width at half maximum (FWHM) of 33.6 meV] of the elastic peak at the clean In/Si(111) surface is changed to the one with the FWHM of 11.5 meV. However, our band structures for the Na-adsorbed 4×2 surface [Fig. 5(a)] show no evidence for the opening of a CDW gap and therefore do not support the metal-insulator transition claimed by Lee *et al.*[4] It is interesting to note in Fig. 5(a) that the band gaps partially open along the $\Gamma X'$ and $M'Y$ symmetry lines by 162 and 156 meV, respectively.[17] These pseudogaps may be related to the loss peak S_c in the HREELS data, which appears to be most prominent at off-specular geometry ($\theta_i=62°$ and $\theta_f=58°$). Although the possibility of S_c being a phonon line was dismissed because of its width,[4] it could, because of the disordered nature of the surface, represent a spread of phonon frequencies. (Note the near equality of the H_1 and H_2 adsorption energies in both the 4×2 and 4×3 structures.)

Finally, we examine the bonding nature of Na atoms on In/Si(111). Comparing Figs. 5(a) and 5(b) with the clean surface energy bands in Fig. 2 of Ref. 7 one sees that, up to 1 ML, Na adsorption simply fills the In-derived surface-state bands without the appearance of Na-derived states near the Fermi energy. Thus, we expect that upon Na adsorption electron transfer occurs from adsorbed Na atoms into In atoms. As expected, our calculated charge density difference defined as

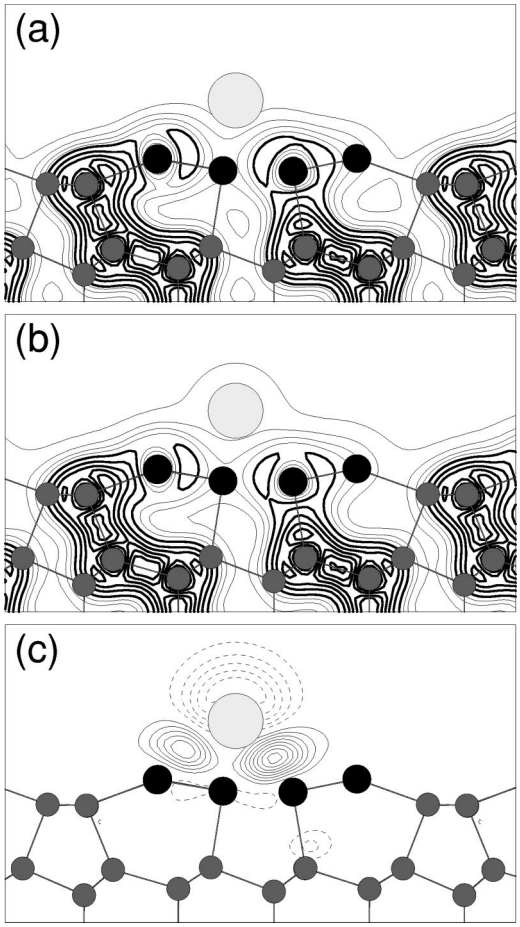

FIG. 6. Contour plots of the charge density in the $[\bar{1}10]$ plane and through the Na atom for (a) the Na-adsorbed 4×2 surface, (b) a superposition of the charge densities of the clean In/Si(111)-(4×2) surface and an isolated half monolayer of Na atoms. The charge density difference between (a) and (b) is given in (c). Two kinds of contour spacings in (a) and (b) are used. The first thin line is at 0.004 e/bohr^3 with spacings of 0.004 e/bohr^3. The first thick line is at 0.02 e/bohr^3 with a spacing of 0.01 between thick lines. In (c) the first solid (dashed) line is at 0.0004 e/bohr^3 (-0.0004 e/bohr^3) with spacings of ±0.0004 e/bohr^3.

$$\Delta\rho=\rho_{\text{Na/InSi}}-(\rho_{\text{InSi}}+\rho_{\text{Na-layer}}) \tag{2}$$

clearly shows that electron charge is transferred mainly from the region on top of the Na atoms into the region above the neighboring In atoms, corresponding to the position of the p_z orbitals of In atoms [see Fig. 6(c)]. Here the charge density of the Na-adsorbed In/Si(111)-(4×2) surface ($\rho_{\text{Na/InSi}}$) and the superposition of the charge densities of the separated systems [clean In/Si(111)-(4×2) (ρ_{InSi}) and isolated half monolayer of Na atoms ($\rho_{\text{Na-layer}}$)], are shown in Figs. 6(a)

and 6(b), respectively. Thus, adsorbed Na atoms become effectively positive ions, giving rise to repulsion between Na atoms and decreasing the work function as manifested above from the calculated adsorption energies and work functions for various Na coverages. This repulsion causes the ion at H_1 (H_2) in Fig. 2 to move to the left (right). Both ions move further off the surface to prevent the decrease in d_3 (Fig. 1) from becomming too large. Thus we see in Table I that at the saturation coverage of 2 ML the interatomic distances d_1 and d_2 significantly increase while d_3 decreases relative to lower coverages.

IV. CONCLUSIONS

Our density-functional total-energy calculations for the adsorption of Na on In/Si(111) surfaces predict the formation of 1D Na wires along the channel between the two zigzag In chains. Our results for the structural and electronic properties of Na wires provide the theoretical basis for the interpretation of the recent LEED, STM, and HREELS data. Our band-structure calculations do not support a metal-insulator transition resulting from a CDW gap induced by the Na adsorbates, but can explain the most of the HREELS spectra which show a significant decrease of the linewidth of the elastic peak and the shift of the S_2 peak with Na adsorption. Our calculated potential-energy surface showed that Na atoms can easily diffuse along the channel between the two In chains, forming a locally 1D Na wire even at low coverages. Thus, it is likely that a finite line of Na atoms in the 4×2 structure would be related to the 4×2 LEED pattern as well as the local 4×2 short-range order observed in the filled-state STM image.

ACKNOWLEDGMENTS

We thank Professor J. W. Chung and Professor H. W. Yeom for providing us their work before publication. J.H.C. thanks Professor K. S. Kim for valuable discussions. This work was supported by the National Science Foundation under Grant No. DMR-0073546, the Welch Foundation (Houston, TX), National Partnership for Advanced Computational Infrastructure at UC San Diego, and the Advanced Computing Center for Engineering and Science (The University of Texas at Austin).

[1] G. Grüner, *Density Waves in Solids* (Addison-Wesley, Reading, MA, 1994).
[2] J.M. Carpinelli, H.H. Weitering, E.W. Plummer, and R. Stumpf, Nature (London) **381**, 398 (1996).
[3] H.H. Weitering, J.M. Carpinelli, A.V. Melechko, J. Zhang, M. Bartkowiak, and E.W. Plummer, Science **285**, 2107 (1999); A.V. Melechko, J. Braun, H.H. Weitering, and E.W. Plummer, Phys. Rev. B **61**, 2235 (2000).
[4] S. S. Lee, J. R. Ahn, N. D. Kim, J. H. Min, C. G. Hwang, J. W. Chung, H. W. Yeom, S. V. Ryjkov, and S. Hasegawa, Phys. Rev. Lett. **88**, 196401 (2002).
[5] H.W. Yeom, S. Takeda, E. Rotenberg, I. Matsuda, K. Horikoshi, J. Schaefer, C.M. Lee, S.D. Kevan, T. Ohta, T. Nagao, and S. Hasegawa, Phys. Rev. Lett. **82**, 4898 (1999).
[6] C. Kumpf, O. Bunk, J.H. Zeysing, Y. Su, M. Nielsen, R.L. Johnson, R. Feidenhans'l, and K. Bechgaard, Phys. Rev. Lett. **85**, 4916 (2000).
[7] J.-H. Cho, D.H. Oh, K.S. Kim, and L. Kleinman, Phys. Rev. B **64**, 235302 (2001).
[8] P. Hohenberg and W. Kohn, Phys. Rev. **136**, B864 (1964); W. Kohn and L.J. Sham, *ibid.* **140**, A1133 (1965).
[9] J.P. Perdew, K. Burke, and M. Ernzerhof, Phys. Rev. Lett. **77**, 3865 (1996); **78**, 1396(E) (1997).
[10] N. Troullier and J.L. Martins, Phys. Rev. B **43**, 1993 (1991).
[11] L. Kleinman and D.M. Bylander, Phys. Rev. Lett. **48**, 1425 (1982).
[12] Although the charge density is negligible at the midpoint, its cube root is not. Therefore the exchange-correlation potential (Refs. 8 and 9) has not quite vanished. Because it does vanish far enough away from the surface, its contribution at the midpoint must be ignored.
[13] Gerald P. Aldredge and Leonard Kleinman, Phys. Rev. Lett. **28**, 1264 (1972); Phys. Rev. B **10**, 559 (1974).
[14] R. I. Masel, *Principles of Adsorption and Reaction on Solid Surfaces* (Wiley, New York, 1996), p. 607.
[15] The H_1 and H_2 4×3 unit cell consists of 1*, 2,1, 2*, 1,2 sites with Na on sites with asterisks whereas the 4×2 consists of 1*, 2*, 1, 2.
[16] Because of the large supercell required to test this explanation, it remains only speculation. Also note that the interchain Coulomb repulsion is expected to be larger for the (4×2) chain than for the (4×3). Therefore the energy difference between isolated (4×2) and (4×3) chains is expected to be slightly less than we have calculated.
[17] These gaps are present in the In/Si(111)-(4×2) surface energy bands but so narrow that we could not identify them in Fig. 2 of Ref. 7.